Since January 2020 Elsevier has created a COVID-19 resource centre with free information in English and Mandarin on the novel coronavirus COVID-19. The COVID-19 resource centre is hosted on Elsevier Connect, the company's public news and information website.

Virology 376 (2008) 357–370

Contents lists available at ScienceDirect

Virology

journal homepage: www.elsevier.com/locate/yviro

Inhibition of alphavirus infection in cell culture and in mice with antisense morpholino oligomers

Slobodan Paessler [a,b,*,1], Rene Rijnbrand [c,1,2], David A. Stein [d], Haolin Ni [a], Nadezhda E. Yun [a], Natallia Dziuba [a], Viktoriya Borisevich [a], Alexey Seregin [a], Yinghong Ma [c], Robert Blouch [d], Patrick L. Iversen [d], Michele A. Zacks [a]

[a] Department of Pathology, University of Texas Medical Branch, 301 University Boulevard, Galveston, TX 77555-1019, USA
[b] Institute for Human Infections and Immunity, University of Texas Medical Branch, Galveston, TX 77555-0609, USA
[c] Department of Microbiology and Immunology, University of Texas Medical Branch, Galveston, TX 77555-1019, USA
[d] AVI BioPharma, Inc., Corvallis, OR 97333, USA

ARTICLE INFO

Article history:
Received 26 December 2007
Returned to author for revision
24 January 2008
Accepted 27 March 2008
Available online 12 May 2008

Keywords:
Venezuelan equine encephalitis virus
Sindbis virus
Pathogenic alphaviruses
Antiviral agents
Antisense therapy
Morpholino oligomers

ABSTRACT

The genus *Alphavirus* contains members that threaten human health, both as natural pathogens and as potential biological weapons. Peptide-conjugated phosphorodiamidate morpholino oligomers (PPMO) enter cells readily and can inhibit viral replication through sequence-specific steric blockade of viral RNA. Sindbis virus (SINV) has low pathogenicity in humans and is regularly utilized as a model alphavirus. PPMO targeting the 5′-terminal and AUG translation start site regions of the SINV genome blocked the production of infectious SINV in tissue culture. PPMO designed against corresponding regions in Venezuelan equine encephalitis virus (VEEV) were likewise found to be effective *in vitro* against several strains of VEEV. Mice treated with PPMO before and after VEEV infection were completely protected from lethal outcome while mice receiving only post-infection PPMO treatment were partially protected. Levels of virus in tissue samples correlated with animal survival. Uninfected mice suffered no apparent ill-effects from PPMO treatment. Thus, PPMO appear promising as candidates for therapeutic development against alphaviruses.

Introduction

The genus *Alphavirus* in the family *Togaviridae* consists of 28 viruses, most of which cycle between mosquito vectors and vertebrate hosts. Several alphaviruses, including Venezuelan equine encephalitis virus (VEEV), Eastern equine encephalitis virus (EEEV), Western equine encephalitis virus (WEEV), O'nyong-nyong virus and Chikungunya virus, can cause severe disease in humans, that typically includes fever and neurological sequelae (Griffin, 2007). Of these, VEEV is the most important human pathogen, with several recent outbreaks consisting of hundreds of thousands of cases occurring mostly in Latin America (Weaver et al., 2004). Furthermore, EEEV, WEEV, and VEEV are considered bioterrorist threats because they cause severe disease in humans, can be produced in large quantity and/or are potentially transmitted by aerosol (Hawley and Eitzen, 2001; Sidwell and Smee, 2003). Veterinary vaccines of varying quality against EEEV, WEEV, and VEEV are commercially available, but only IND preparations are approved for human use and their availability is limited to military and laboratory personnel. No therapeutic for alphavirus-induced disease exists, although supportive treatment and anti-inflammatory drugs may be beneficial. Recently short interfering RNAs (siRNAs) have been shown to be effective against the alphaviruses Semliki Forest virus (Caplen et al., 2002) and VEEV (O'Brien, 2006), in cell cultures, and against O'nyong-nyong virus replication in its natural mosquito vector, *Anopheles gambiae* (Keene et al., 2004).

Alphaviruses have a single positive-stranded RNA genome of approximately 12 kb that codes for two polyproteins that are processed to four nonstructural proteins and three structural proteins, respectively. The open reading frames are flanked by 5′ and 3′ untranslated regions (UTRs) of approximately (~) 60 and ~300 nucleotides, respectively. The nonstructural proteins are translated from the full-length genomic RNA and are utilized to produce a full-length negative-strand antigenomic RNA. The negative-strand intermediate is used as template to produce both full-length positive-strand, and, using a 24 nucleotide internal promoter, a ~4 kb subgenomic RNA is produced, which is identical in sequence to the 3′ terminal third of the genomic RNA. The structural proteins are translated from the subgenomic RNA. Both genomic and subgenomic RNA are 5′ capped and 3′ polyadenylated. Sindbis virus (SINV) has been extensively used as a model alphavirus because of its low

* Corresponding author. Department of Pathology, University of Texas Medical Branch, 301 University Boulevard, Galveston, TX 77555-1019, USA. Fax: +1 409 747 0762.
E-mail address: slpaessl@utmb.edu (S. Paessler).
[1] These authors contributed equally to this work.
[2] Current address: Itherx, 10790 Roselle Street, San Diego, CA, USA.

0042-6822/$ – see front matter © 2008 Elsevier Inc. All rights reserved.
doi:10.1016/j.virol.2008.03.032

pathogenicity to humans, easy propagation in a variety of cell lines, and molecular biology that is considered representative of the genus (Strauss and Strauss, 1994).

Antisense oligomers of various structural types have been used to interfere with gene expression of several human viral pathogens (Schubert and Kurreck, 2006), and a phosphorothioate oligonucleotide designed to target mRNA of cytomegalovirus (CMV) that is intended to treat CMV-induced retinitis is an approved drug (De Clercq, 2004). However, antisense therapeutic technology continues to be hampered by limitations in both oligomer stability and delivery to RNA targets within relevant cells (Kurreck, 2003). Phosphorodiamidate morpholino oligomers (PMO) are a class of oligonucleotide-like antisense agents that possess the same four bases as DNA, but contain a different backbone. The deoxyribose ring and phosphodiester linkage of DNA are replaced by a morpholine ring and phosphorodiamidate linkage in PMO (Summerton and Weller, 1997). PMO are nonionic, are stable in cellular extracts and human serum (Nelson et al., 2005; Youngblood et al., 2007) and typically are synthesized to a length of 20–25 subunits. The PMO mechanism of antisense action is via steric-blocking of complementary RNA sequence (Stein et al., 1997), and thus differs from that of antisense agents based on DNA chemistry, which induce RNase H-mediated cleavage of the RNA strand of a RNA–DNA duplex, or RNAi/siRNA involving double-stranded agents that recognize target mRNA and induce its degradation by cellular proteins (Masiero et al., 2007). PMO covalently conjugated to a cell-penetrating peptide (CPP) can be delivered efficiently into cells (Deas et al., 2005; Moulton et al., 2004; Yuan et al., 2006; Zhang et al., 2006). CPP-PMO are water-soluble and have been shown to generate potent inhibition of several RNA viruses, including dengue virus (Holden et al., 2006; Kinney et al., 2005), West Nile virus (Deas et al., 2005), SARS Coronavirus (Neuman et al., 2005), Equine Arterivirus (van den Born et al., 2005) and influenza virus (Ge et al., 2006) in cell culture, and Coxsackievirus B3 (Yuan et al., 2006), Ebola virus (Enterlein et al., 2006), murine Coronavirus (Burrer et al., 2007) and West Nile virus (Deas et al., 2007) both in cell culture and in mouse models. Two different CPP-conjugated PMO (PPMO), one containing oligoarginine (P3) and one containing 6-aminohexanoic acid (P7), have been utilized (Moulton et al., 2004; Abes et al., 2006). A recent report documented that P7-conjugated PPMO are highly stable in human serum for at least 2 hours (h), and moderately stable for 24 h (Youngblood et al., 2007).

In the present study, we first evaluated six SINV-specific PPMO designed to base pair with sequences in the four terminal regions of the full-length genome or antigenome, the AUG translation start site region of the polyprotein coding sequence for the nonstructural proteins, and the subgenomic promoter region of the negative-strand antigenome. We found that two PPMO, one targeting the 5′-terminal sequence and the other targeting the first functional AUG translation start site regions of the genome, were effective in blocking viral production. Subsequently, PPMO were designed to target the two corresponding regions in VEEV. As for the SINV PPMO, VEEV-specific PPMO were found to inhibit the replication of several VEEV strains in cell cultures and were efficacious in a murine model of VEE.

Results

Design of PPMO

Considerations in PPMO sequence design for this study included our current understanding of the function of various alphavirus genetic regions, and PPMO mechanism of action. As with other positive-strand viruses that utilize cap-dependent translation, access of trans-acting proteins to the 5′ terminal region of the genome is critical to alphavirus capping reactions and the process of translation pre-initiation (Vasiljeva et al., 2000). It has also been shown by mutational studies that certain sequence and secondary structure requirements in the 5′ terminal region of the alphavirus genome must be present for efficient viral replication to occur (Frolov et al., 2001; Gorchakov et al., 2004; Niesters and Strauss, 1990; Tsiang et al., 1988). The 3′ terminal region of the antigenome has likewise been shown to play an integral role in positive-strand synthesis (Frolov et al., 2001), perhaps through the presence of a stem-loop structure corresponding to the inverse of that present in the 5′ end of the genome. Specific sequence requirements in the 19 nucleotide 3′ conserved sequence element (3′CSE) immediately preceding the polyA tail are necessary for efficient minus-strand synthesis (Frolov et al., 2001). Another study reported high antiviral activity from PPMO targeting the 5′ terminal region of the Equine Arterivirus genome, and moderate activity with PPMO targeting either the 3′ terminus of the genome or 3′ terminus of the antigenome (van den Born et al., 2005), although the 5′ end of the antigenome was not included as a target. Other groups have also reported high efficacy by PPMO targeting the genomic 5′ terminal region of other positive-strand viruses, including dengue (Kinney et al., 2005), West Nile virus (Deas et al., 2005), porcine reproductive and respiratory syndrome virus (Zhang et al., 2006) and murine Coronavirus (Burrer et al., 2007). The above reports documenting the importance of sequence and structures in terminal regions of the alphavirus genome, along with the

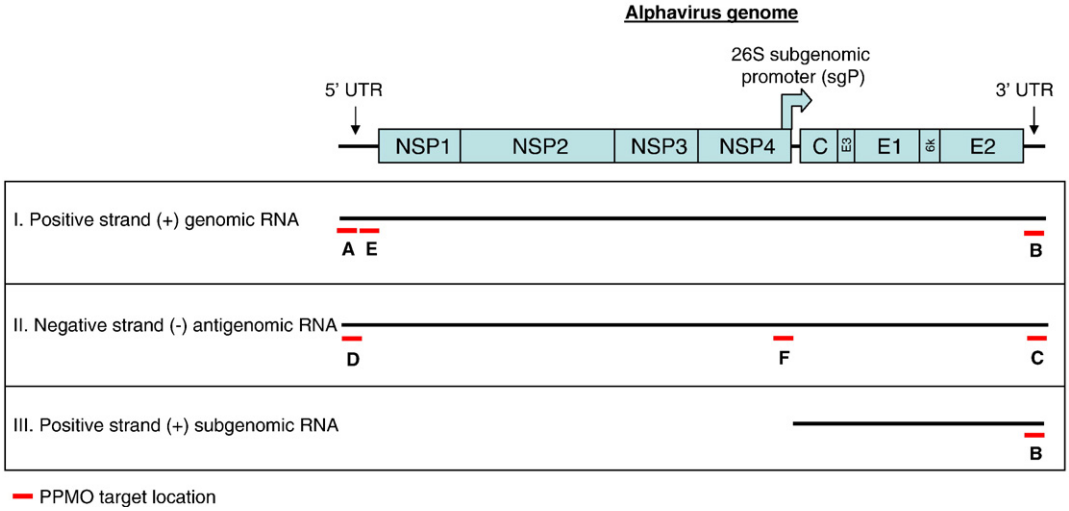

Fig. 1. Location of PPMO target sites in alphavirus genome segments. A schematic representation of the alphavirus genome is shown. PPMO were designed to target the terminal 5′ and 3′ untranslated regulatory regions (UTR) of alphavirus genomic (+) and antigenomic (−) RNA (labeled A–D), as well as the AUG translation start site region of the genomic (labeled E), and subgenomic promoter region of the antigenomic (labeled F), RNA. Sindbis virus (SINV)- and Venezuelan equine encephalitis virus (VEEV)-specific PPMO name designations and sequences are shown in Table 1.

success of termini-targeted PPMO, led us to design PPMO against each of the four termini of SINV genomic RNA (Fig. 1). Alphavirus subgenomic (sg) RNA encoding the structural proteins is synthesized by internal initiation on the genome-length negative-strand RNA. The minimal sequence essential for promoter activity extends from nucleotide −19 to +5 (in relation to the start codon of the sg positive-strand) and corresponds to the genomic positive-strand sequence from nucleotides 7579 to 7602 in SINV (Levis et al., 1990). We therefore targeted this core-promoter region in the antigenome, in an effort to interfere with the synthesis of plus-strand sg RNA. The genomic 5′-most AUG codon is required for translation initiation of the nonstructural proteins of alphaviruses (Lemm et al., 1994). The region flanking the translation start site has been a favored target site for PMO mediated silencing of viral (Enterlein et al., 2006; Neuman et al., 2005; van den Born et al., 2005) and cellular (Heasman, 2002; Nasevicius and Ekker, 2000) mRNAs, and was an obvious PPMO target selection. Three of the six sites we initially chose to target with PPMO are regions of highly conserved sequence either between alphavirus species, or between strains within a species: (i) the CSE at the 3′ terminus of the genome (ii) the sg core-promoter region and (iii) the 5′ terminal region (Lemm et al., 1994).

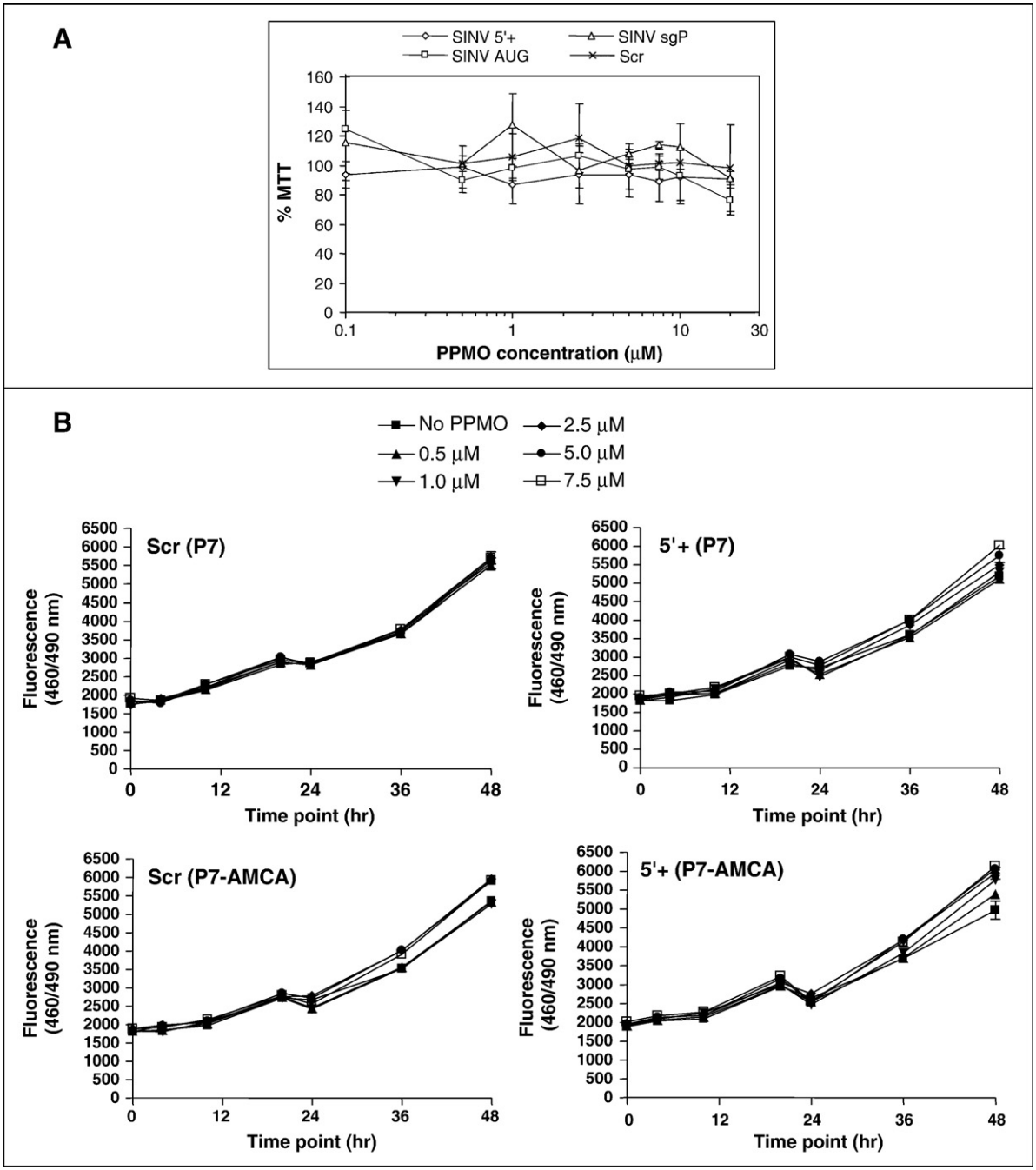

Fig. 2. Effect of PPMO on cell viability. A) SINV PPMO. BHK cells were incubated with the 0.1, 0.5, 1, 2.5, 5, 7.5, 10, or 20 μM of the indicated with the P3-conjugated SINV-specific PPMO (SINV 5′+, SINV AUG, or SINV sgP, see Table 1), or as a negative control, the P3-conjugated Scr PPMO (a random nucleotide sequence), for 24 h. Reduction of cell viability, measured by MTT assay (described in Materials and methods), is expressed relative to mock-treated cells. B) VEEV PPMO. Vero cells were incubated with the P7- or P7-AMCA-conjugated VEEV 5′+ PPMO (see Table 1), or as a negative control, the P7- or P7-AMCA-conjugated Scr PPMO (a random nucleotide sequence) with a range of PPMO concentrations (0.1, 0.5, 1, 2.5, 5 and 7.5 μm) and for different time points (0, 4, 10, 20, 24, 36, 48 h). The average of quadruplicate treatments, measured by CellTiter-Blue® assay (described in Materials and methods), is shown. Two-way ANOVA (α=0.05) with Bonferroni post-test for pairwise comparison of PPMO-treated vs. untreated ("No PPMO") controls by respective time point and concentration was performed.

PPMO are minimally cytotoxic

The impact of P3-PPMO on cell viability was evaluated by MTT assay on BHK cells following 24 h incubation with the P3-conjugated PPMO – SINV 5′+, SINV AUG, SINV sgP, and Scr – in the range of 0.1–20 μM (Fig. 2A). Cell viability readings for all PPMO at all concentrations tested, relative to vehicle-treated cells, were ~80% or greater. Similar cytotoxicity evaluation was carried out for the P7- and the P7-AMCA-conjugated PPMO (VEEV 5′+ and Scr) (Fig. 2B). Viability assay was performed in quadruplicate at multiple time points (0, 4, 10, 20, 24, 36 and 48 h) and concentrations (0.5, 1.0, 2.5, 5.0, and 7.5 μM) using a fluorescence-based assay. For the majority of time points, there were minimal differences (± 2%) in cell viability in comparison to the untreated (no PPMO) control at the matching time point; for either the P7- or P7-AMCA-conjugated VEEV 5′+ PPMO at a given treatment/time point, this reduction in viability did not exceed 10%. For the majority of the PPMO incubations, no statistically significant decrease in viability was detected in two way ANOVA (α=0.05) with Bonferroni pairwise comparison to the untreated control ("No PPMO") at the matching concentration and time point, with the exception of the VEEV 5′+ (P7), and the Scr (P7-AMCA) at the 1 μM concentration/24h time point (9% reduction in viability for both).

Two PPMO efficiently inhibit recombinant alphavirus production in vitro

To assess if these PPMO could successfully inhibit alphavirus replication, as well as to confirm the utility of the recombinant full-length Sindbis virus which expresses the luciferase (luc) reporter protein (SinLuc) as a tool for monitoring anti-SINV compounds, we evaluated SINV-targeting PPMO (Table 1) in this system. SinLuc virus was harvested following electroporation of BHK cells with *in vitro* transcribed SinLuc RNA. Prior to infection with SinLuc virus BHK cells were treated with SINV P3-PPMO in the concentration range that was demonstrated to be non-cytotoxic in the cell viability experiment (shown in Fig. 2A). For quantitative comparison, statistical analysis was performed to evaluate the luc levels for all groups (PPMO or untreated control at all concentrations via two way ANOVA, α=0.05) as well as pairwise comparison of luc levels for SINV PPMO treatments or untreated ("No PPMO") at each concentration to the corresponding Scr treatment (Bonferroni's post-test, α=0.05). Dose-responsive inhibition of SINV replication, as represented by luc readings, was observed for both the SINV 5′+ PPMO (Fig. 3A, right panel) and SINV AUG PPMO (3A, left panel). For the SINV AUG PPMO, at 5, 7.5 and 10 μM this reduction was in the range of 70–90% relative to Scr and was statistically significant (p-values<0.01). For the SINV 5′+, a reduction of 85–100% with the dose tested in the range of 0.5–10 μM was significant (p-values<0.001). In contrast, the level of inhibition produced by the SINV 5′-, 3′+ and 3′- PPMO was similar at all concentrations, and these levels were significantly different from Scr PPMO (p-values<0.01); however, this reduction (%) did not appear to be dose dependent. For the SgP, no significant differences were detected at the majority of the concentrations tested, with the exception of 0.1 and 7.5 μM. However, at 0.1 μM, for all groups (PPMO or untreated controls), the luc values were generally higher relative to Scr, but were not statistically different from Scr (p-values>0.05). Thus, significant dose-responsive inhibition was observed for the SINV 5′+ and SINV AUG PPMO.

Table 1
PPMO sequences and target locations

Legend[a]	PPMO	Sequence (5′ to 3′)	Region of PPMO target location
A	SINV 5′+[b]	CAATAGTGTGTACTACGCCGTC	5′ terminus of SINV genome
B	SINV 3′+[b]	GTTAAAAACAAAATTTTGTTG	3′ terminus of SINV genome
C	SINV 5′–[b]	CAACAAAATTTTGTTTTTAAC	5′ terminus of SINV antigenome
D	SINV 3′–[b]	GACGGCGTAGTACACACTATTG	3′ terminus of SINV antigenome
E	SINV AUG[b]	GGCTTCTCCATTGTGATGGTAG	AUG of SINV genome
F	SINV sgP[b]	CTCTATTCATGGTGGTGGTGT	Subgenomic promoter of SINV antigenome
A	VEEV 5′+[c,d]	GCTTCTCTCATGCGCCGCCCAT	5′ terminus of VEEV genome
E	VEEV AUG[c]	GAACTTTCTCCATTTTGGGTAG	AUG of VEEV genome
–	Scr[d,e]	AGTCTCGACTTGCTACCTCA	Random sequence
–	HRV 5′+[b]	CAAAGGTACATAGTACCAGAG	5′ terminus of HRV genome
–	HRV CRE[b]	GTCTGTTTCGTTTTCTCAACG	Cis-acting replication element (CRE) of HRV

[a] The letter designations indicate the target location in the alphavirus genome, as shown in Fig. 1.
[b] PPMO conjugated to P3 peptide.
[c] PPMO conjugated to P7 peptide.
[d] PPMO conjugated to P7 and to 7-amino-4-methylcoumarin-3-acetic acid (AMCA).
[e] PPMO conjugated to either P3 or P7 peptide.

PPMO inhibit infectious Sindbis virus production in vitro

To assess the ability of PPMO to inhibit production of infectious alphavirus in cell culture, BHK cell infection with wild type SINV (Fig. 3B, panels i) was performed under conditions similar to those used for the SinLuc virus experiments (shown in Fig. 3A). SINV-infected BHK cells were incubated with SINV 5′+, SINV AUG, SINV sgP, or SINV 3′+ PPMO and virus production level was determined by plaque assay of supernatants obtained at 24 hpi (Fig. 3A). A statistically significant reduction in titer resulted from SINV 5′+ and SINV AUG PPMO treatment (Dunnett's test of PPMO vs. mock treatment, p<0.01 for each); at 1 μM, a reduction of 86% and 88% was measured for SINV 5′+ and SINV AUG, respectively; at 5 μM, the level of inhibition was higher (p<0.01): 99% and 89%, respectively. In contrast, SINV sgP and SINV 3′+ PPMO did not affect the SINV levels significantly (p>0.05).

To further assess the virus specific effects of the two SINV-specific PPPMO that inhibited viral production in these prior experiments, Vero cells were infected at an moi of 0.1 with the control viruses, VSV and VEEV (TC-83), and then incubated with the SINV AUG and SINV 5′+ PPMO at a concentration of 5 μM, or as a control, Vero cell were infected, but left untreated ("no PPMO", Fig. 3B, panel ii). For VSV, titers were most variable at the earlier time point of 8 h, with a maximum difference in titer from the untreated control of 1.4 $\log_{10}$ PFU/ml (SINV AUG); at the later time point of 24 h, VSV titers were similar for all the PPMO, with a maximum difference of 0.71 $\log_{10}$ PFU/ml. For TC83, titers were more consistent at 8 h, with maximum difference of ~1 $\log_{10}$ PFU/ml; at 24 h, the maximum difference was ~2 $\log_{10}$ PFU/ml. No obvious trend in non-specific inhibition by any of these PPMO was evident.

PPMO directed at 5′ sequence elements inhibit SINV translation

The effect of PPMO on viral translation was assessed following SINV 5′+, SINV AUG, SINV sgP or SINV 3′+ PPMO treatment of SINV-infected cell cultures. Quantification of the level of viral capsid (C) and envelope (E1) proteins in ^{35}S-labeled BHK cell lysates obtained at 24 hpi and resolved by SDS-PAGE indicates that the SINV 5′+ and the SINV AUG PPMO strongly inhibited viral translation, with capsid protein expression at 1.2% and 16% of the infected, untreated cells (Fig. 3C). In contrast, incubation with the SINV sgP and SINV 3′+ PPMO produced little inhibition of viral translation, with capsid expression at 92% and 86%, respectively, relative to the infected, mock-treated cells. These results are consistent with the SINV 5′+ or SINV AUG PPMO-mediated inhibition of recombinant (SinLuc, Fig. 3A) and wild type SINV (Fig. 3B).

PPMO are potent inhibitors of viral translation

In vitro transcribed SINV RNA was used to program rabbit reticulocyte lysate (Fig. 3D) in the presence of different ratios of molar excess of SINV (Fig. 3D, panel i) and human rhinovirus type 14 (HRV14)-specific PPMO (Fig. 3D, panel ii). None of the HRV14 specific PPMO inhibited SINV-driven translation. These results were identical to that observed for two other HRV-targeting PPMO (R. Rijnbrand,

manuscript in preparation). In contrast, the SINV 3′+ and SINV sgP PPMO did not inhibit viral translation. SINV 5′+ and AUG showed strong inhibition of viral translation with SINV AUG, even inhibiting at a 1:1 molar ratio. SINV 5′+ inhibited translation, but less efficiently than the other PPMO tested, with some detectable protein expression still evident in the presence of 10-fold molar excess.

PPMO inhibition of VEEV production in vitro

Based on the observed anti-SINV effectiveness of the SINV 5′+ and SINV AUG PPMO against SINV in the above experiments, PPMO designed to target the corresponding regions of VEEV were then synthesized (Fig. 1). While the SINV PPMO had been synthesized with P3 as the peptide component of the PPMO, the two VEEV-specific antisense and the Scr control sequences were prepared as P7-PPMO. The more-recently developed P7 was selected as the conjugation peptide for the VEEV experiments, as it has been reported to transport PPMO into cells with equal or greater ability than that provided by P3 peptide (Abes et al., 2006), yet is more stable (Youngblood et al., 2007), less affected by serum (Deas et al., 2005) and less cytotoxic than P3 (Abes et al., 2006).

Vero cells were infected with various strains of VEEV or, as a control, with VSV, prior to the addition of VEEV 5+, VEEV AUG or Scr PPMO (Fig. 4A) at 5 μM. At 8 (left panel) or 24 hpi (right panel), the supernatant was harvested for analysis of viral titer via plaque assay. At both time points, viral titers of the VEEV 5+ or VEEV AUG-treated cultures were below the limit of detection (0.6 $\log_{10}$ PFU/ml) for all VEEV strains. In contrast, for the VSV control, viral production was relatively unaffected by PPMO treatment; VSV levels were in the range of 2–3 $\log_{10}$/ml and 5–8 $\log_{10}$ PFU/ml at 8 and 24 hpi, respectively. The relative virus production for the different VEEV strains was similar at both time points, however, the titers at 24 h were ~5 $\log_{10}$ higher. These experiments indicate that the VEEV 5′+ PPMO was effective at reducing the virus production at 8 and 24 hpi for multiple strains of VEEV, despite a moderate level of non-specific activity. Dose–response experiments with TC83 were subsequently performed at the same moi and incubation time, but including additional sampling time points and concentrations using the VEEV 5′+ P7-PPMO conjugated to the fluorescent label, AMCA (Fig. 4B), or as control, the P7-AMCA-conjugated Scr. At the lower doses of 0.5 and 1.0 μM, no significant reduction in viral titer was detected for the 5′+ PPMO-treated cells in comparison to Scr. However, the 5′+ PPMO treatment resulted in a modest reduction at a dose of 2.5 μM, and marked reduction at doses of 5, 7.5 and 10 μM. No reduction in the virus production pattern was observed for Scr-treated cells compared to untreated VEEV-infected cells at any of the concentrations or time points tested.

To assess the robust nature of the observed qualitative differences in inhibition by the VEEV PPMO, additional analysis of the effects on VEEV (TC-83) was performed (Fig. 4C). Vero cells were infected with VEEV or, as a control, with VSV, for 1 h (+1 h) prior to the addition of VEEV 5+, VEEV AUG or Scr PPMO at 5 μM. Supernatants were collected at 8 and 24 h for determination of the level of virus production via plaque assay, which was performed in eight replicates. A statistically significant difference in titer level was detected between VEEV 5′+ PPMO and VEEV AUG in pairwise comparison to either the Scr or untreated ("No PPMO") control (Bonferroni, $p<0.001$); for VEEV 5′+, a reduction of 65–68% and 43–45% was detected at 8 and 24 h, respectively, whereas a more modest reduction of 23–29% and 21–24% was detected for VEEV AUG at these time points (Fig. 4C, panel ii). At 8 h, a small (but statistically significant) titer increase was detected for Scr treatment in comparison to untreated ("No PPMO"), however, there was no significant difference at 24 h ($p<0.05$).

Treatment of combined VEEV 5′+ and VEEV AUG was evaluated at two concentrations, 7.5 mM and 10 μM (each PPMO), as shown in Fig. 4D. Vero cells were infected with VEEV (TC-83) or, as a control, with VSV, for one h (+1 h) prior to the addition of the combined VEEV. Supernatants were collected at 8 and 24 h (and for VSV, at 48 h) for determination of the level of virus production. For the treatments with combined VEEV PPMO, the percent inhibition relative to VEEV-infected, untreated Vero cells ("No PPMO"), as shown in the table (Fig. 4D, bottom), was similar at both time points and concentrations; 48–51% for 5 μM of each PPMO and 46–48 for 7.5 μM of each. In contrast, for VSV, overall lower percent inhibition resulted from treatment with combined PPMO; 4 and 13% inhibition at 8 and 24 h, respectively, for 5 μM (each PPMO), and 6 and 4% inhibition, respectively, at 8 and 24 h for 10 μM (each PPMO); no substantial difference were seen at 48 h (no inhibition and 6% inhibition for 5 and 10 μM).

Combined intranasal and subcutaneous PPMO treatment protects mice against lethal VEEV infection

The animal model of VEEV using infection of NIH Swiss mice by the highly virulent ZPC738 strain is well-described (Paessler et al., 2003, 2006). Mice develop encephalitis/paralysis and typically succumb to disease between 6 and 10 days post-infection. Our prior experience with intranasal delivery of vaccines against VEEV in mice (Anishchenko et al., 2006; Ni et al., 2007) suggested to us that a novel administration route of PPMO using a combination of intranasal and subcutaneous delivery would potentially be effective against neuroinvasive viruses such as VEEV. Other studies have reported that the use of 200 μg/dose (10 mg/kg) delivered via intraperitoneal (i.p.) against WNV (Deas et al., 2007) or via intravenous (i.v.) route against coxsackievirus B3 virus (Yuan et al., 2006) was nontoxic and provided antiviral effects.

We evaluated the antiviral efficacy of combined VEEV 5′+ and VEEV AUG PPMO treatment by measurement of survival and viral titers in the brain and peripheral organs (Fig. 5) of mice receiving treatment with PPMO prior to (+pre) or following (+post) infection with 10^3 PFU of virulent VEEV. No deaths occurred in the group of uninfected mice receiving VEEV-specific PPMO before and after infection (8/8, 100% survival), indicating that this dosing regimen was well-tolerated. In the VEEV-infected groups, there were no survivors in the group receiving both pre- and post-infection treatment with Scr PPMO (0%, 0/10). In contrast, 100% (8/8) of the group receiving both pre- and post-infection treatment with VEEV 5+ and VEEV AUG PPMO survived while 63% (5/8) of the group receiving only post-infection treatment with the VEEV-specific PPMO survived. There was a statistically significant difference among all survival curves (logrank, $p<0.0001$). Statistical comparison of survival between the group receiving PPMO treatment both before and after infection and the untreated VEEV-infected control showed a statistically significant difference ($\alpha=0.05$; Fisher's Exact, $p=0.0002$), as did the group receiving PPMO treatment only after infection, in comparison with the untreated VEEV-infected control group ($\alpha=0.05$; Fisher's Exact, $p=0.0256$).

Infectious virus levels in the brain and peripheral organs of VEEV-infected mice are reduced following combined pre- and post-infection PPMO treatment

We evaluated the VEEV titers at three early post-infection time points (2, 3 and 4 dpi) in the brain and peripheral organs of four randomly selected mice that were treated with i) PPMO diluent (mock treatment), ii) VEEV 5′+ PPMO before and after infection, and iii) VEEV 5′+ PPMO after infection (Fig. 5B). At all time points tested, VEEV was undetectable in the blood, brain, and peripheral tissues (liver, lung and spleen) of mice that received the VEEV 5′+ PPMO pre- and post-infection (+pre/+post) treatments. In mice that received only post-infection (−pre/+post) 5′+ PPMO treatment, reduction in VEEV titer varied, depending upon the tissue examined. In the blood, VEEV titers for the VEEV 5′+ treated groups were similar to those of the mock-treated mice at days 2 and 3 pi, but over 2 logs lower than mock-

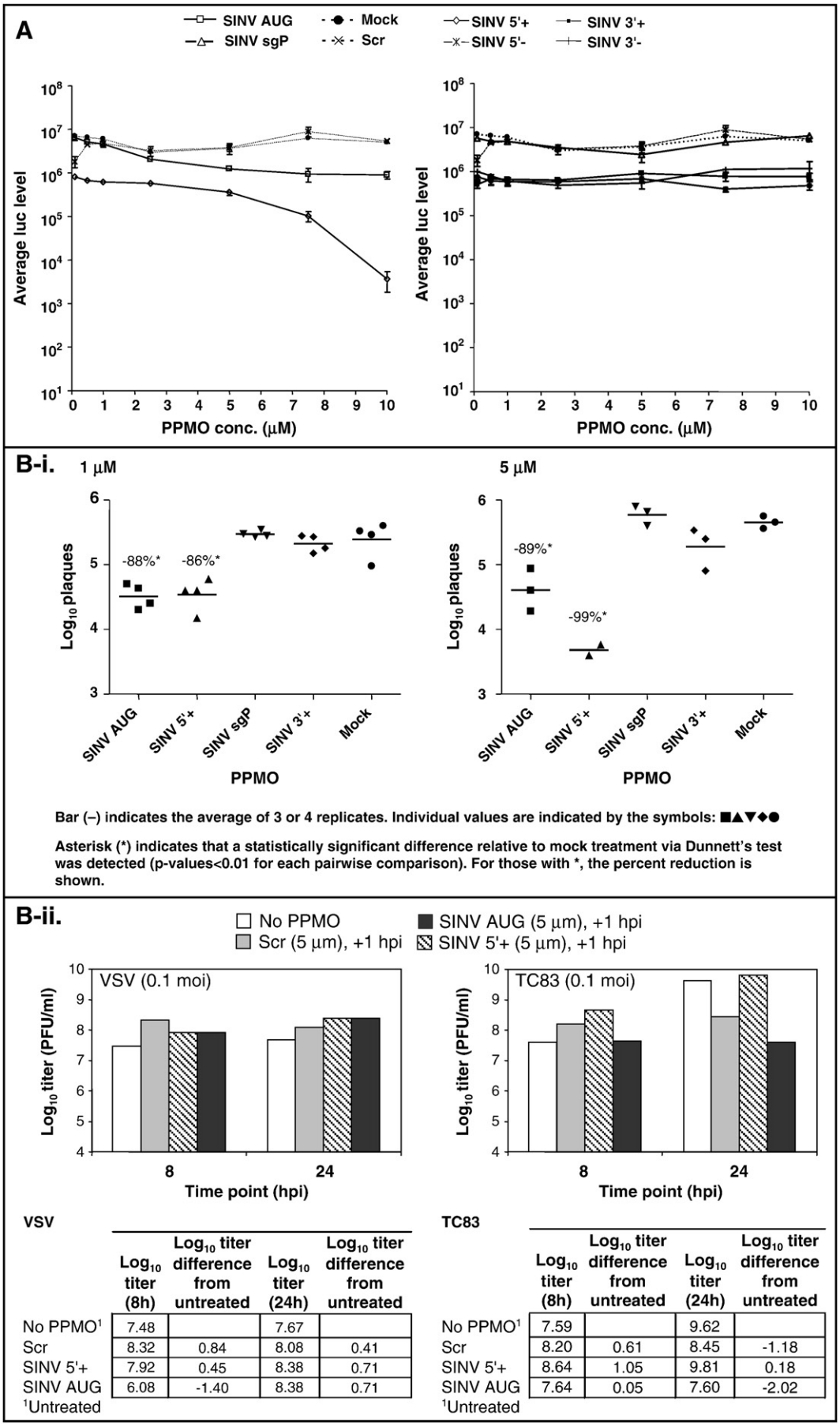

VSV

	Log_{10} titer (8h)	Log_{10} titer difference from untreated	Log_{10} titer (24h)	Log_{10} titer difference from untreated
No PPMO[1]	7.48		7.67	
Scr	8.32	0.84	8.08	0.41
SINV 5'+	7.92	0.45	8.38	0.71
SINV AUG	6.08	-1.40	8.38	0.71

[1]Untreated

TC83

	Log_{10} titer (8h)	Log_{10} titer difference from untreated	Log_{10} titer (24h)	Log_{10} titer difference from untreated
No PPMO[1]	7.59		9.62	
Scr	8.20	0.61	8.45	-1.18
SINV 5'+	8.64	1.05	9.81	0.18
SINV AUG	7.64	0.05	7.60	-2.02

[1]Untreated

Fig. 3.

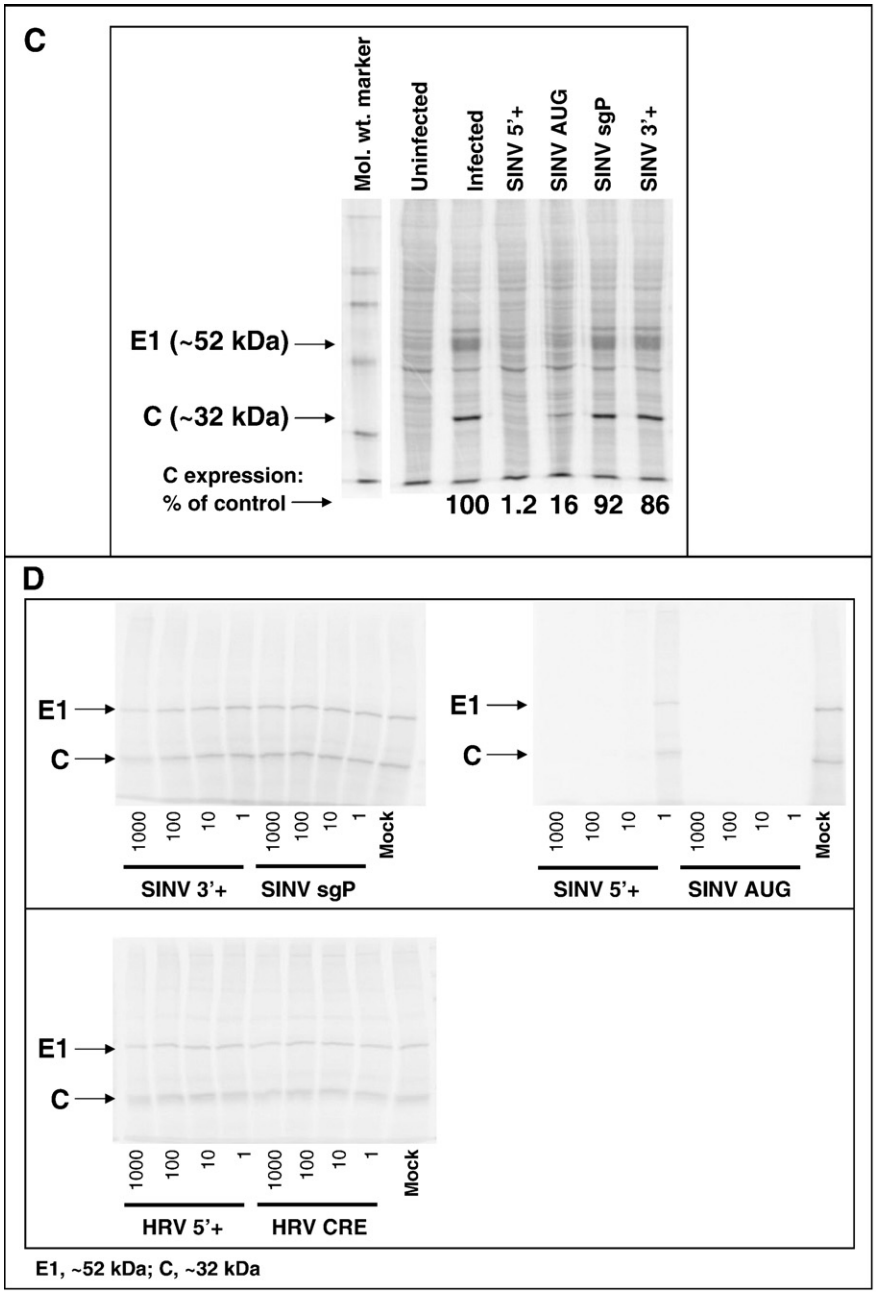

Fig. 3. PPMO antiviral activity against the alphavirus, SINV. A) Dose–response inhibition of recombinant SINV production. BHK cells were infected with SinLuc at a multiplicity of infection (moi) of ~0.03, followed by treatment with the indicated concentrations of SINV AUG, SINV sgP or Scr PPMO (left) or SINV genomic termini targeting PPMO (right) for 24 h. Luciferase (Luc) levels were measured in triplicate, as described in Materials and methods. The average and standard deviation are shown. Statistical analysis of luciferase levels of SINV PPMO vs. Scr treatment (two-way ANOVA, $\alpha = 0.05$; pairwise comparison via Bonferroni post-test) was performed and results are described in the text. B) Dose–response inhibition of wild type SINV. Panel i–ii) Effect of SINV PPMO on SINV production. BHK cells were infected with SINV at an moi of ~0.03 and treated at 1 hpi with the indicated PPMO (1 or 5 μM, panels i and ii, respectively). At 24 hpi, the virus levels in supernatant samples were determined by plaque assay. Supernatants were analyzed in quadruplicate (1 μM) or triplicate (5 μM). The results of one representative experiment out of two performed is shown. Statistical analysis was performed using one-way ANOVA ($\alpha = 0.05$) with Dunnett's Multiple Comparison Test in pairwise comparison of each PPMO-treated group relative to the mock control. Statistically significant differences in Dunnett's test are indicated by an asterisk (*p-value < 0.01) and the percent reduction is shown. Panel iii) Effect of SINV PPMO on two control viruses, VSV and TC83. Vero cells were infected with VSV or VEEV (TC83) at an moi of 0.1 and treated at 1 hpi with the indicated PPMO at 5 μM. At 8 and 24 h, the virus production levels were determined by plaque assay. Viral titration of untreated, infected Vero cells ("No PPMO") was also performed. The result of a single experiment is shown. C) Inhibition of viral protein expression by SINV-specific PPMO. BHK cells were treated with the indicated PPMO starting at 1 h after infection with SINV (moi of 0.03). At 24 hpi the cells were incubated with ^{35}S-methionine for 1 h, and cell lysates then analyzed by SDS-PAGE. The molecular weight marker is shown. Viral capsid (C) and envelope protein (E1) and apparent molecular mass are indicated by the arrows. The percentage of C expression, relative to the mock-treated control, as determined by densitometry, is shown numerically under the lanes. D) Inhibition of viral translation by SINV-specific PPMO. *In vitro* transcribed SINV RNA was translated in rabbit reticulocyte lysates in the presence of a molar excess of the indicated PPMO as described in Materials and methods. Samples were separated by SDS-PAGE and visualized by phosphor imager.

treated on day 4 (Fig. 5B, panel i). In the brain, the VEEV 5′+ group treated following infection (−pre/+post) showed higher titer at day 2, but lower titer at days 3 and 4 compared to the mock-treated group (Fig. 5B, panel ii); notably, on 4 dpi, VEEV titers for the −pre/+post VEEV 5′+ PPMO was reduced to 80 PFU/g tissue, a level near the limit of detection in this assay of 60 PFU/g. Compared to mock-treated mice, the average liver titers in the mice receiving −pre/+post VEEV 5′+ PPMO following infection was about 1 $\log_{10}$ higher at 2 dpi, and about 2 $\log_{10}$ less at 3 and 4 dpi, (Fig. 5B, panel iii). Spleen titers in the group receiving VEEV 5′+ treatment following infection were similar to

mock-treated mice at 2 dpi, somewhat lower than mock at 3 dpi, and considerably lower (undetectable) than mock at 4 dpi (Fig. 5B, panel iv). Lung titers were similarly low for mice treated −pre/+post VEEV with 5′+ and mock-treated mice at 2 and 3 dpi, while at 4 dpi, mock-treated mice had an average titer of ~4 $\log_{10}$ while both PPMO treatment groups had undetectable titers (Fig. 5B, panel v).

Discussion

VEEV is a highly lethal alphavirus that is of considerable human and veterinary health importance. No effective human vaccine or therapeutic against VEEV is presently available. Alphaviruses exhibit robust replication in both cell culture and in animals, and, as such, provide an excellent system to investigate the antiviral efficacy and specificity of PPMO. Here we have demonstrated the potent inhibition of both SINV and a variety of VEEV strains in cell culture with PPMO targeted to the 5′ region of the genomic RNA. Importantly, we were able to prevent VEEV-induced lethal encephalitis in a mouse model.

In this study, we used an alphavirus of low pathogenicity to humans, Sindbis virus, to guide our design of PPMO against the highly pathogenic VEEV. The strategy was successful, as PPMO designed to target the corresponding sequence-regions in VEEV were highly effective *in vitro* and *in vivo* against VEEV. Furthermore, results with a luciferase-expressing SINV showed that the SINV-specific PPMO were strong inhibitors of viral replication (Fig. 3A). The obtained results were consistent with results using wild type SINV (Fig. 3B), validating the utility of SinLuc as a drug screening reagent.

Of the six PPMO designed against SINV, only the two targeting the 5′ region of genomic RNA were effective at inhibiting viral replication. The antiviral efficacy of PPMO targeted to various locations in the 5′ end of the genome of positive-strand RNA viruses has been observed for Nidoviruses (Neuman et al., 2005; van den Born et al., 2005; Zhang et al., 2006), Flaviviruses (Deas et al., 2005; Kinney et al., 2005), and Picornaviruses (Vagnozzi et al., 2007; Yuan et al., 2006). It remains undetermined why four of the six SINV PPMO in this study were relatively ineffective. Future studies may evaluate other regions of alphavirus sequence as prospective PPMO targets, including the 5′ terminal- and AUG-regions of the subgenomic RNA. Results from cell culture (Fig. 3C) and in cell-free translation assays (Fig. 3D) indicate that both active PPMO identified in this study can directly interfere with viral translation. The lack of activity by several PPMO incidentally provides confirmation of the specificity of the inhibitory action of the effective PPMO. In addition, these experiments did not reveal any non-specific toxicity associated with PPMO chemistry, which would be reflected in overall lowered luciferase (Fig. 3A), plaque (Fig. 3B), or viral protein production (Fig. 3C) in comparison with untreated or Scr controls. Further evidence of the lack of toxicity of this compound is provided by cell viability assays for all PPMO used (Fig. 2), the relatively low inhibitory activity of VEEV-specific PPMO against VSV (Fig. 4A), the control (Scr) PPMO employed throughout this study, and the uncompromised health of PPMO-treated (uninfected) mice (Fig. 5A).

Both the VEEV 5′+ and AUG PPMO were highly effective against multiple strains of VEEV in cell culture (Fig. 4A). This is not surprising, considering the high to perfect sequence conservation of the PPMO target sites among the VEEV strains tested. Similar sequence conservation is present in all the VEEV strains available from GenBank (data not shown), and indicates that these two PPMO may represent a useful antiviral treatment for enzootic as well as epidemic strains of VEEV. Studies designed to target the corresponding conserved sequences in two other major groups of encephalitic alphaviruses, EEEV and WEEV, are currently in progress.

Complete protection was provided against otherwise lethal VEEV-induced disease in the murine model when antisense PPMO were administered both before and after infection. However, post-infection PPMO treatment conferred partial protection, indicating that PPMO may be useful even in a strictly therapeutic setting. Tissue titer data (Fig. 5B) reflected the survival profiles (Fig. 5A) in the mouse efficacy experiment, and clearly implicates reduction in virus production as the mechanism of efficacy of the antisense PPMO. The novel PPMO administration scheme employed in this study (subcutaneous combined with intranasal) is deserving further exploration, as it may be that modification of the relative proportions and doses of PPMO delivered by these two inoculation routes could be fine-tuned to further enhance efficacy. Notably, the two modes of administration employed here are preferable to intravenous injection for prospective human treatment. It will also be of interest to explore PPMO efficacy against VEEV strains other than ZPC738 in this same mouse model, or against VEEV in other animal models.

Materials and methods

Preparation of PPMO

All PMO were synthesized at AVI BioPharma Inc. (Corvallis, OR) by methods previously described (Summerton and Weller, 1997). SINV-specific PMO were covalently conjugated, at the 5′ end, to the arginine-rich peptide NH_2-R_9F_2C-$CONH_2$ (abbreviated 'P3'), and VEEV-specific PMO to NH_2-$(RXR)_4XB$-$CONH_2$ (X=6-aminohexanoic acid, B=Beta alanine) (abbreviated 'P7'). The conjugation, purification and analysis of PPMO were performed by procedures previously described (Abes et al., 2006; Moulton et al., 2004). Additionally, P7-PPMO versions of the VEEV 5+ and Scr were prepared with the fluor AMCA (7-amino-4-methyl-3-coumarinyl acetic acid; Sigma-Aldrich, St. Louis, MO) conjugated to the 3′ end by methods similar to those described previously for carboxyfluorescein conjugation to PMO (Moulton et al., 2003).

Design of specific PPMO

PPMO of 21–22 bases in length were designed to target, by complementary base pairing, regions in SINV or VEEV that have been identified as important in the viral RNA synthesis or translation. The

Fig. 4. PPMO antiviral activity against pathogenic alphaviruses. A) PPMO inhibition of multiple VEEV strains. Vero cells were infected at a moi of 0.1 with the indicated strain of VEEV (TC-83, SH3, ZPC738, or 68U201) or, as a negative control, with vesicular stomatitis virus (VSV) for 2 h prior to the addition of the indicated PPMO at 5 μM. At 8 (left) or 24 hpi (right), supernatants were harvested for analysis of viral titer via plaque assay. The VEEV serotype is indicated in parentheses. SH3 and TC-83 are epizootic (or epizootic derivative) strains; 68U201 and ZPC738 are enzootic strains. The horizontal line depicts the limit of detection. Asterisk (*) indicates that no virus was detected for any sample in that group. The result of a single experiment is shown. B) PPMO dose–response inhibition of VEEV. Vero cells were infected at a moi of 0.1 with VEEV (TC-83 strain) for 1 h prior to the addition of the indicated P7-AMCA-conjugated PPMO at doses in the range of 0.5 to 10 μM. At various time points post-infection (indicated in graph), supernatants were harvested for analysis of viral titer via plaque assay. The result of a single experiment is shown. C) Effect of VEEV PPMO on VEEV and on the control virus, VSV (eight replicates). Vero cells were infected at a moi of 0.1 with VEEV (TC-83 strain), or as a control, with VSV, for 1 h prior to the addition of the indicated P7-AMCA-conjugated PPMO at 5 μM. Supernatants were harvested at 8 and 24 hpi for analysis of viral titer via plaque assay, performed in eight replicates at each time point for VEEV or VSV. Statistical analysis was performed on $\log_{10}$-transformed viral titer values comparing all treatments using one-way analysis of variance (α=0.05, GraphPad Prism). Pairwise comparison of the $\log_{10}$-titer values by treatment group was performed using Bonferroni post-test. Bars with asterisk indicate a statistically significant difference (Bonferroni, p-value<0.001). The average percent change was calculated from $\log_{10}$ titers as: 100*(VEEV PPMO-average control)÷average control. A summary table showing the average percent change, relative to either the untreated ("No PPMO") or Scr controls is shown. D) Effect of combined VEEV 5′+ and VEEV AUG PPMO on VEEV. Vero cells were infected at a moi of 0.1 with VEEV (TC-83 strain), or as a control, with VSV, for 1 h prior to the addition of the indicated P7-AMCA-conjugated PPMO at 7.5 and 10 μM (each PPMO). Supernatants were harvested at 8 and 24 hpi (and for VSV, at 8, 24, and 48 hpi) for analysis of viral titer via plaque assay. The result of a single experiment is shown.

PPMO sequences and name designations are specified in Table 1 and a schematic representation of their target locations is provided in Fig. 1. Additionally, a 20-mer PMO of random sequence having 50% G/C content (named 'Scr') was conjugated to either P3 or P7 peptide for use as a control for non-sequence-specific activity of the two respective PPMO chemistries. To preclude unintentional hybridization events, antisense and negative control PPMO sequences were screened via BLAST (http://www.ncbi.nlm.nih.gov/BLAST/) against primate and murine mRNA sequences. In addition, the negative control was screened against all published alphavirus sequences. PPMO targeted to human rhinovirus type 14 (HRV14) were used as additional controls for SINV *in vitro* translation experiments. Prior to use, lyophilized PPMO were suspended with filter-sterilized distilled water to a concentration of 1–2 mM, and stored at 4 °C.

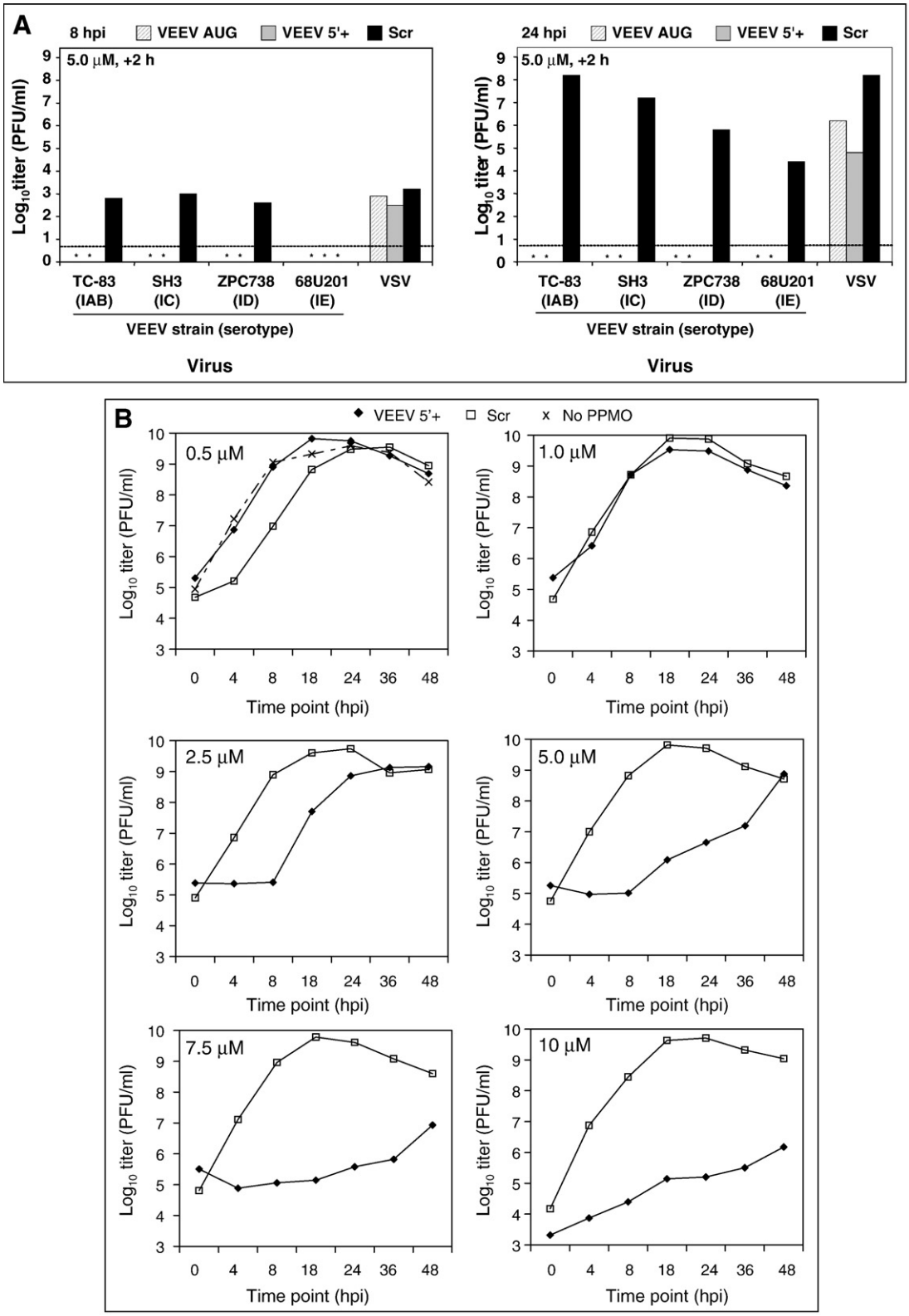

Fig. 4.

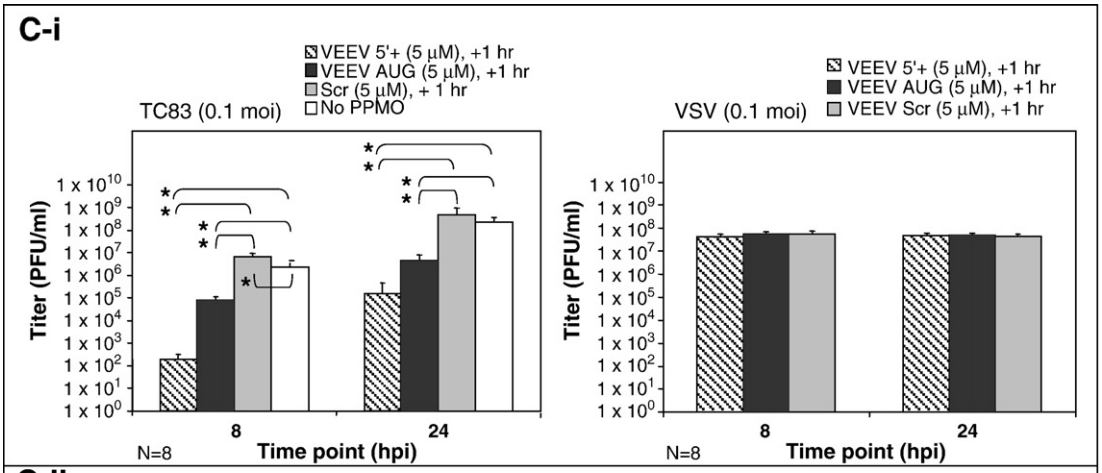

C-ii

PPMO (Conc.), Time added	Supernatant time point (hpi)	Percent change: Relative to untreated control – Average	Relative to untreated control – SD	Relative to Scr – Average	Relative to Scr – SD
VEEV 5'+ (5 μM), +1 hr	8	-65%	4.4%	-68%	4.1%
	24	-43%	7.3%	-45%	7.1%
VEEV AUG (5 μM), +1 hr	8	-23%	3.3%	-29%	3.1%
	24	-21%	4.6%	-24%	4.5%
Scr (5 μM), + 1 hr	8	7%	2.4%	--	
	24	3%	5.2%	--	

*Statistically significant difference (grey fill). For data shown in Fig. 3C. panel i, statistical analysis was performed for each time point using one-way ANOVA (α=0.05) with Bonferroni Multiple Comparison Test (relative to untreated ("No PPMO") control, or to Scr, as indicated). Summary is shown for VEEV. For the control virus, VSV, no significant differences were detected (not shown). SD, standard deviation.

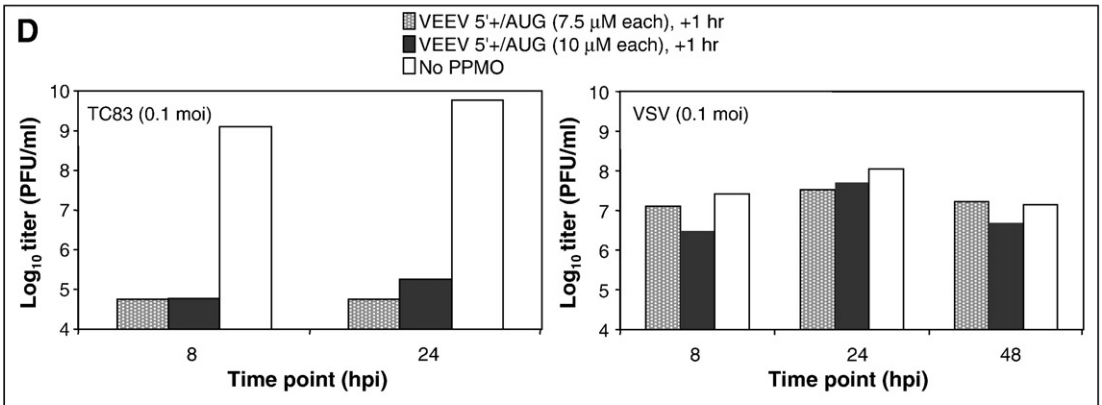

PPMO (Conc.), Time added	Supernatant time point (hpi)	Percent change relative to untreated[1] for indicated virus: VEEV	VSV
VEEV 5'+/AUG (7.5 μM each), +1 hr	8	-47.9%	-4.1%
	24	-51.4%	-6.3%
	48	N.D.	1.2%
VEEV 5'+/AUG (10 μM each), +1 hr	8	-47.6%	-12.6%
	24	-46.3%	-3.9%
	48	N.D.	-6.4%

[1]No PPMO

N.D., not done

Fig. 4 (*continued*).

Viruses

The following VEEV strains were used: ZPC738 (Roehrig and Bolin, 1997; Wang et al., 1999), TC-83 (Berge et al., 1961; Kinney et al., 1989), SH3 (Rico-Hesse et al., 1995), and 68U201 (Oberste et al., 1996; Scherer et al., 1970). Alphavirus stocks were generated by growth in cell culture and the viral titer of the stock was obtained via plaque assay, as described previously (Paessler et al., 2003).

Sindbis virus (SINV, TE12) was obtained by electroporation of BHK cells with RNA derived from pTOTO1101 (Rice et al., 1987). A clone containing an infectious copy of SinLuc was a gift from Ilya Frolov (UTMB). Vesicular stomatitis virus (VSV) was obtained from Scott Weaver.

Cells

The baby hamster kidney cell line, BHK21 (BHK), (American Type Culture Collection, Manassas, VA) and Vero cells were maintained at 37 °C, 5% CO_2 in Dulbecco's Modified Eagle's Medium (DMEM, Hyclone, Logan, UT) with 10% fetal bovine serum and antibiotics.

Viability assay

For the P3-conjugated SINV-specific PPMO, spectrophotometric measurement of the reduction of MTT (3-(4,5-Dimethylthiazol-2-yl)-2,5-diphenyltetrazolium bromide) to formazan was performed according to the manufacturer's protocol (Sigma, St. Louis, MO) (Mosmann, 1983). BHK cells at 80% confluency were incubated with the indicated PPMO in the range of 0.1–20 μM for 24 h. The production of formazan relative to mock-treated cells was used to assess PPMO toxicity. For the P7- and P7-AMCA-conjugated VEEV-specific (VEEV 5′+ or VEEV AUG) and the control (Scr) PPMO, viability assay measuring the conversion of resazurin to resorufin was performed using CellTiter-Blue® Reagent (Promega, Madison, WI). Briefly, Vero cells were incubated with PPMO concentrations in the range of 0–7.5 μM for 1 h, after which the incubation media was removed and cells incubated for various time periods (0, 4, 10, 20, 24, 36 and 48 h). Each treatment was performed in quadruplicate wells. At the designated time point, 20 μl of CellTiter-Blue was added to each well. Plates were then incubated in accordance with the manufacturer's recommendations, and read on a Bio-Tek FLx800 fluorescent plate reader ($560_{Ex}/590_{Em}$nm).

In vitro inhibition of SINV replication

In vitro transcription of pSinLuc and electroporation of RNA into BHK cells was performed to generate viral stocks for infection, as described previously (Liljestrom and Garoff, 1991). BHK cells were infected with SINV or SinLuc at a multiplicity of infection (moi) of ~0.03 and treated at 1 h post-infection (hpi) with the indicated PPMO. The cells were then incubated for 24 h and virus production was determined via plaque assay of virus production or via quantitative luciferase assay (Promega, Madison, WI). *In vitro* translation reactions were performed using rabbit reticulocyte lysate (Promega), as described by the supplier. Lysates were programmed with 125 ng RNA/10 μl lysate and were resolved by SDS-PAGE and analyzed by phosphor imager. Statistical analysis of the average luciferase levels obtained from triplicate measurement was performed using two-way analysis of variance (ANOVA, α=0.05) with pairwise comparison of each SINV PPMO with Scr using Bonferroni's post-test using GraphPad Prism 4.0 (GraphPad Software, San Diego California USA). Statistical analysis of the level of virus production ($\log_{10}$ transformed) obtained from quadruplicate (1 μM) or triplicate (5 μM) values was performed using one-way ANOVA (α=0.05) with Dunnett's Multiple Comparison Test for pairwise comparison of each PPMO-treated group to the mock-treated control (GraphPad Prism 4.0). To further evaluate potential non-specific effects of the SINV PPMO, experiments were performed using Vero cells infected with VSV or VEEV (TC-83) at an moi of 0.1 and then treated with the SINV 5′+, SINV AUG or Scr PPMO at 1 h post-infection (+1 h). Cell supernatants were harvested at 8 and 24 hpi for determination of viral titer via plaque assay. In parallel, supernatants were also collected from untreated, infected Vero cells ("No PPMO") for viral titration.

Viral protein expression

BHK cells were infected with SINV at an moi of 0.03 and treated with PPMO at 1 hpi. ^{35}S-methionine was added to cells at 24 hpi and cells harvested 1 h later. Cell lysates were prepared by detergent lysis and analyzed by SDS-PAGE (10%) followed by densitometry (Storm 840 gel imaging system). Viral proteins were identified (E1, ~52kDa; C, ~32kDa) using a ^{14}C labeled molecular weight marker (Amersham Life Science, Arlington Heights, IL), as published previously (Paessler et al., 2003).

In vitro inhibition of VEEV replication

Vero cells were infected at a moi of 0.1 with the indicated strain of VEEV (TC-83, SH3, ZPC738, or 68U201), or, as a negative control, with VSV and incubated for 1–2 h (+1 or +2 h, as indicated in the figure legends) prior to the addition of the indicated VEEV PPMO (AUG, VEEV 5′+, or Scr). Virus containing media was removed and the indicated PPMO was added at a concentration of 5 μM. Supernatant was harvested at 8 or 24 hpi for analysis of viral titer via plaque assay (Paessler et al., 2003). Statistical analysis of virus titers ($\log_{10}$ transformed) obtained from eight replicate values (where indicated in figure legend) was performed using one-way ANOVA (α=0.05) with Bonferroni's Multiple Comparison Test for pairwise comparison of each group. Combined PPMO treatment was performed as described above. Briefly, Vero cells were infected at a moi of 0.1 with the indicated strain of VEEV (TC-83), or as a control, with VSV, and incubated for +1 h prior to the addition of 7.5 or 10 μM (each PPMO) of combined VEEV AUG and VEEV 5′+. As a control, untreated Vero cells were incubated in parallel. Plaque assay of supernatants obtained at 8, 24, and 48 h (the latter for VSV only) was performed.

Mice

Nine-week-old NIH Swiss mice were purchased from Harlan Sprague Dawley, Inc. (Indianapolis, IN), and allowed to acclimatize for at least 1 week. All studies were approved by the UTMB Institutional Animal Care and Use Committee and work with VEEV was performed at the Biosafety Level-3 in accordance with UTMB Health and Safety approval and guidelines. Mice were allowed food and water ad libitum throughout the studies.

PPMO efficacy in mice

Mice were treated with VEEV-specific PPMO (combined AUG and 5′+ in equal amounts) or the random control PPMO (Scr) in serum-free DMEM at a dose per mouse of 40 μg via i.n. route and 160 μg via s.c. route at time points pre- (2 doses: − 24 h and − 4 h, indicated as "+pre") and/or post-infection (5 doses: daily on day +1 through +5, indicated as "+post"). On day 0, the indicated groups were infected with 10^3 PFU of virulent VEEV (ZPC738) via i.n. route. Control groups consisted of the following: 1) VEEV-specific PPMO-treated, VEEV-infected mice, and 2) VEEV-infected, but untreated mice. Mice (N=8–10 per group) were monitored daily for death over a 28-day period following infection. At 2, 3 and 4 days post-infection (dpi), four animals per group were euthanized for harvest of blood, brain and peripheral organs (liver, spleen and lung). Infectious virus levels in the tissues were determined via plaque assay, as described previously (Paessler et al., 2003). Statistical analysis of survival for all groups over the indicated period was performed using logrank test at a significant level of α<0.05 in GraphPad® Prism (San Diego, CA). For pairwise comparison of the survival of treated and untreated (or mock-treated) groups Fisher's Exact Test was performed at a significance level of α<0.05 in GraphPad® Prism.

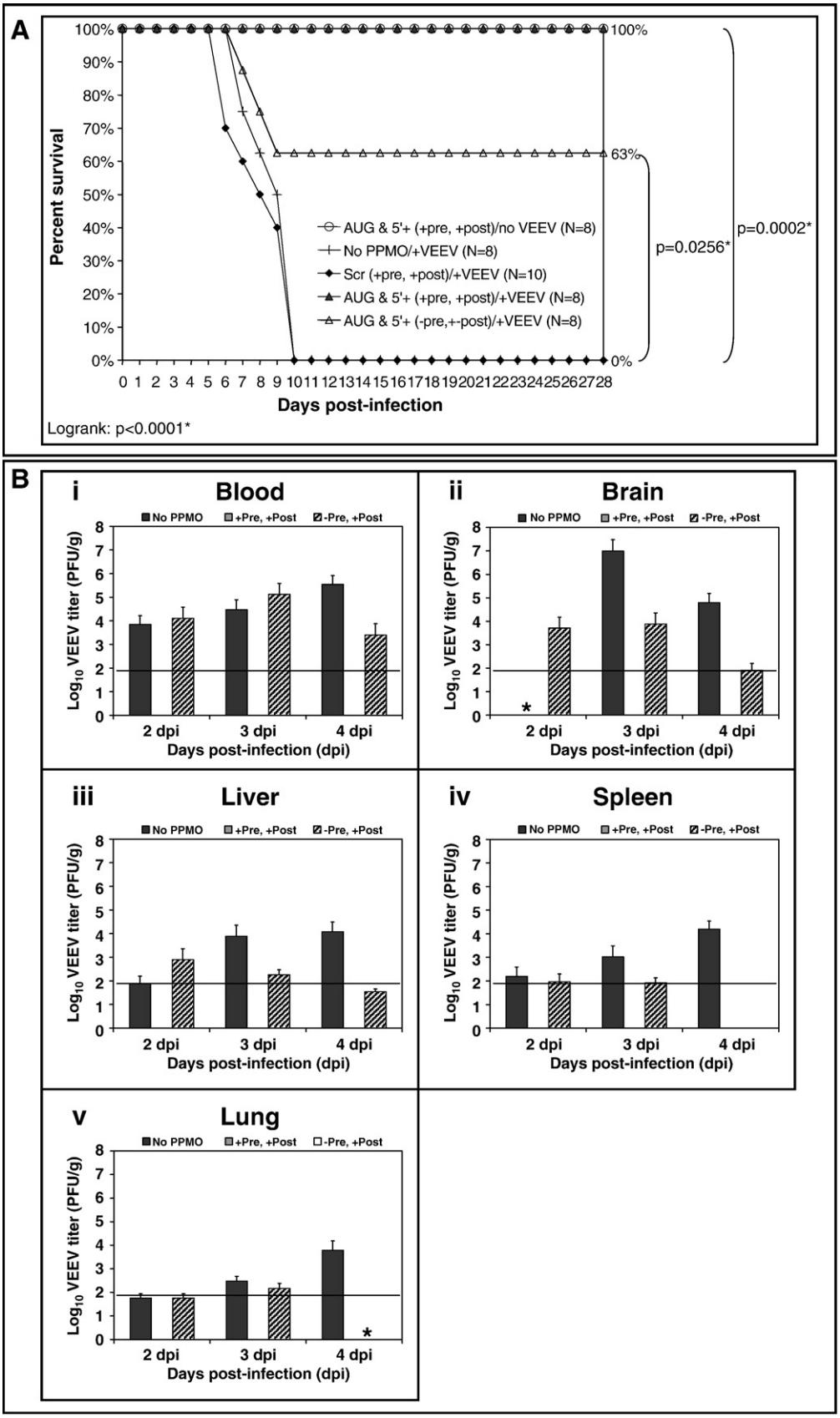
A
Percent survival
100%
90%
80%
70%
60%
50%
40%
30%
20%
10%
0%
0 1 2 3 4 5 6 7 8 9 10 11 12 13 14 15 16 17 18 19 20 21 22 23 24 25 26 27 28
Days post-infection
AUG & 5'+ (+pre, +post)/no VEEV (N=8)
No PPMO/+VEEV (N=8)
Scr (+pre, +post)/+VEEV (N=10)
AUG & 5'+ (+pre, +post)/+VEEV (N=8)
AUG & 5'+ (-pre,+-post)/+VEEV (N=8)
100%
63%
0%
p=0.0256*
p=0.0002*
Logrank: p<0.0001*
B
i Blood
ii Brain
iii Liver
iv Spleen
v Lung
No PPMO
+Pre, +Post
-Pre, +Post
Log10 VEEV titer (PFU/g)
2 dpi
3 dpi
4 dpi
Days post-infection (dpi)
*

Fig. 5.

Acknowledgments

The authors wish to thank The Chemistry Group at AVI BioPharma for the expert production of all PPMO compounds used in this study. This work was supported by grants from the National Institute of Allergy and Infectious Diseases through the Western Regional Center of Excellence for Biodefense and Emerging Infectious Diseases Research (U54 AI057156) and through the Galveston National Laboratory Operations, Advanced Veterinary Services Core (UC7 AI070083). S. Paessler was supported by a National Institutes of Health K08 Award (A1059491) and faculty support provided by the Institute for Human Infections and Immunity at UTMB. We thank Jenna Linde for exceptional assistance with data entry and preparation of figures.

References

Abes, S., Moulton, H.M., Clair, P., Prevot, P., Youngblood, D.S., Wu, R.P., Iversen, P.L., Lebleu, B., 2006. Vectorization of morpholino oligomers by the (R-Ahx-R)(4) peptide allows efficient splicing correction in the absence of endosomolytic agents. J. Control. Release 116 (3), 304–313.

Anishchenko, M., Bowen, R.A., Paessler, S., Austgen, L., Greene, I.P., Weaver, S.C., 2006. Venezuelan encephalitis emergence mediated by a phylogenetically predicted viral mutation. Proc. Natl. Acad. Sci. U. S. A. 103 (13), 4994–4999.

Berge, T.O., Banks, I.S., Tigertt, W.D., 1961. Attenuation of Venezuelan equine encephalomyelitis virus by in vitro cultivation in guinea pig heart cells. Am. J. Hyg. 73, 209–218.

Burrer, R., Neuman, B.W., Ting, J.P., Stein, D.A., Moulton, H.M., Iversen, P.L., Kuhn, P., Buchmeier, M.J., 2007. Antiviral effects of antisense morpholino oligomers in murine Coronavirus infection models. J. Virol. 81 (11), 5637–5648.

Caplen, N.J., Zheng, Z., Falgout, B., Morgan, R.A., 2002. Inhibition of viral gene expression and replication in mosquito cells by dsRNA-triggered RNA interference. Mol. Ther. 6 (2), 243–251.

De Clercq, E., 2004. Antivirals and antiviral strategies. Nat. Rev. Microbiol. 2 (9), 704–720.

Deas, T.S., Binduga-Gajewska, I., Tilgner, M., Ren, P., Stein, D.A., Moulton, H.M., Iversen, P.L., Kauffman, E.B., Kramer, L.D., Shi, P.Y., 2005. Inhibition of flavivirus infections by antisense oligomers specifically suppressing viral translation and RNA replication. J. Virol. 79 (8), 4599–4609.

Deas, T.S., Bennett, C.J., Jones, S.A., Tilgner, M., Ren, P., Behr, M.J., Stein, D.A., Iversen, P.L., Kramer, L.D., Bernard, K.A., Shi, P.Y., 2007. In vitro resistance selection and in vivo efficacy of morpholino oligomers against West Nile virus. Antimicrob. Agents Chemother. 51 (7), 2470–2482.

Enterlein, S., Warfield, K.L., Swenson, D.L., Stein, D.A., Smith, J.L., Gamble, C.S., Kroeker, A.D., Iversen, P.L., Bavari, S., Muhlberger, E., 2006. VP35 knockdown inhibits Ebola virus amplification and protects against lethal infection in mice. Antimicrob. Agents Chemother. 50 (3), 984–993.

Frolov, I., Hardy, R., Rice, C.M., 2001. Cis-acting RNA elements at the 5′ end of Sindbis virus genome RNA regulate minus- and plus-strand RNA synthesis. Rna 7 (11), 1638–1651.

Ge, Q., Pastey, M., Kobasa, D., Puthavathana, P., Lupfer, C., Bestwick, R.K., Iversen, P.L., Chen, J., Stein, D.A., 2006. Inhibition of multiple subtypes of influenza a virus in cell cultures with morpholino oligomers. Antimicrob. Agents Chemother. 50 (11), 3724–3733.

Gorchakov, R., Hardy, R., Rice, C.M., Frolov, I., 2004. Selection of functional 5′ cis-acting elements promoting efficient sindbis virus genome replication. J. Virol. 78 (1), 61–75.

Griffin, D.E., 2007. Alphaviruses, In: Knipe, D.M., Howley, P.M. (Eds.), Fifth Edition. Fields' Virology, 2. Lippincott, Williams and Wilkins, Philadelphia, pp. 917–962.

Hawley, R.J., Eitzen Jr., E.M., 2001. Biological weapons—a primer for microbiologists. Annu. Rev. Microbiol. 55, 235–253.

Heasman, J., 2002. Morpholino oligos: making sense of antisense? Dev. Biol. 243 (2), 209–214.

Holden, K.L., Stein, D.A., Pierson, T.C., Ahmed, A.A., Clyde, K., Iversen, P.L., Harris, E., 2006. Inhibition of dengue virus translation and RNA synthesis by a morpholino oligomer targeted to the top of the terminal 3′ stem-loop structure. Virology 344 (2), 439–452.

Keene, K.M., Foy, B.D., Sanchez-Vargas, I., Beaty, B.J., Blair, C.D., Olson, K.E., 2004. RNA interference acts as a natural antiviral response to O'nyong-nyong virus (Alphavirus; *Togaviridae*) infection of *Anopheles gambiae*. Proc. Natl. Acad. Sci. U. S. A. 101 (49), 17240–17245.

Kinney, R.M., Johnson, B.J., Welch, J.B., Tsuchiya, K.R., Trent, D.W., 1989. The full-length nucleotide sequences of the virulent Trinidad donkey strain of Venezuelan equine encephalitis virus and its attenuated vaccine derivative, strain TC-83. Virology 170 (1), 19–30.

Kinney, R.M., Huang, C.Y., Rose, B.C., Kroeker, A.D., Dreher, T.W., Iversen, P.L., Stein, D.A., 2005. Inhibition of dengue virus serotypes 1 to 4 in vero cell cultures with morpholino oligomers. J. Virol. 79 (8), 5116–5128.

Kurreck, J., 2003. Antisense technologies. Improvement through novel chemical modifications. Eur. J. Biochem. 270 (8), 1628–1644.

Lemm, J.A., Rumenapf, T., Strauss, E.G., Strauss, J.H., Rice, C.M., 1994. Polypeptide requirements for assembly of functional Sindbis virus replication complexes: a model for the temporal regulation of minus- and plus-strand RNA synthesis. EMBO J. 13 (12), 2925–2934.

Levis, R., Schlesinger, S., Huang, H.V., 1990. Promoter for Sindbis virus RNA-dependent subgenomic RNA transcription. J. Virol. 64 (4), 1726–1733.

Liljestrom, P., Garoff, H., 1991. A new generation of animal cell expression vectors based on the Semliki Forest virus replicon. Biotechnology (N.Y.) 9 (12), 1356–1361.

Masiero, M., Nardo, G., Indraccolo, S., Favaro, E., 2007. RNA interference: implications for cancer treatment. Mol. Aspects Med. 28 (1), 143–166.

Mosmann, T., 1983. Rapid colorimetric assay for cellular growth and survival: application to proliferation and cytotoxicity assays. J. Immunol. Methods 65 (1–2), 55–63.

Moulton, H.M., Hase, M.C., Smith, K.M., Iversen, P.L., 2003. HIV Tat peptide enhances cellular delivery of antisense morpholino oligomers. Antisense Nucleic Acid Drug Dev. 13 (1), 31–43.

Moulton, H.M., Nelson, M.H., Hatlevig, S.A., Reddy, M.T., Iversen, P.L., 2004. Cellular uptake of antisense morpholino oligomers conjugated to arginine-rich peptides. Bioconjug. Chem. 15 (2), 290–299.

Nasevicius, A., Ekker, S.C., 2000. Effective targeted gene 'knockdown' in zebrafish. Nat. Genet. 26 (2), 216–220.

Nelson, M.H., Stein, D.A., Kroeker, A.D., Hatlevig, S.A., Iversen, P.L., Moulton, H.M., 2005. Arginine-rich peptide conjugation to morpholino oligomers: effects on antisense activity and specificity. Bioconjug. Chem. 16 (4), 959–966.

Neuman, B.W., Stein, D.A., Kroeker, A.D., Churchill, M.J., Kim, A.M., Kuhn, P., Dawson, P., Moulton, H.M., Bestwick, R.K., Iversen, P.L., Buchmeier, M.J., 2005. Inhibition, escape, and attenuated growth of severe acute respiratory syndrome Coronavirus treated with antisense morpholino oligomers. J. Virol. 79 (15), 9665–9676.

Ni, H., Yun, N.E., Zacks, M.A., Weaver, S.C., Tesh, R.B., da Rosa, A.P., Powers, A.M., Frolov, I., Paessler, S., 2007. Recombinant alphaviruses are safe and useful serological diagnostic tools. Am. J. Trop. Med. Hyg. 76 (4), 774–781.

Niesters, H.G., Strauss, J.H., 1990. Defined mutations in the 5′ nontranslated sequence of Sindbis virus RNA. J. Virol. 64 (9), 4162–4168.

O'Brien, L., 2006. Inhibition of multiple strains of Venezuelan equine encephalitis virus by a pool of four short interfering RNAs. Antivir. Res. 1–10.

Oberste, M.S., Parker, M.D., Smith, J.F., 1996. Complete sequence of Venezuelan equine encephalitis virus subtype IE reveals conserved and hypervariable domains within the C terminus of nsP3. Virology 219 (1), 314–320.

Paessler, S., Fayzulin, R.Z., Anishchenko, M., Greene, I.P., Weaver, S.C., Frolov, I., 2003. Recombinant sindbis/venezuelan equine encephalitis virus is highly attenuated and immunogenic. J. Virol. 77 (17), 9278–9286.

Paessler, S., Ni, H., Petrakova, O., Fayzulin, R.Z., Yun, N., Anishchenko, M., Weaver, S.C., Frolov, I., 2006. Replication and clearance of Venezuelan equine encephalitis virus from the brains of animals vaccinated with chimeric SIN/VEE viruses. J. Virol. 80 (6), 2784–2796.

Rice, C.M., Levis, R., Strauss, J.H., Huang, H.V., 1987. Production of infectious RNA transcripts from Sindbis virus cDNA clones: mapping of lethal mutations, rescue of a temperature-sensitive marker, and in vitro mutagenesis to generate defined mutants. J. Virol. 61 (12), 3809–3819.

Rico-Hesse, R., Weaver, S.C., de Siger, J., Medina, G., Salas, R.A., 1995. Emergence of a new epidemic/epizootic Venezuelan equine encephalitis virus in South America. Proc. Natl. Acad. Sci. U. S. A. 92, 5278–5281.

Roehrig, J.T., Bolin, R.A., 1997. Monoclonal antibodies capable of distinguishing epizootic from enzootic varieties of Subtype I Venezuelan equine encephalitis viruses in a rapid indirect immunofluorescence assay. J. Clin. Microbiol. 35 (7), 1887–1890.

Scherer, W.F., Dickerman, R.W., Ordonez, J.V., 1970. Discovery and geographic distribution of Venezuelan encephalitis virus in Guatemala, Honduras, and British Honduras during 1965–68, and its possible movement to Central America and Mexico. Am. J. Trop. Med. Hyg. 19 (4), 703–711.

Schubert, S., Kurreck, J., 2006. Oligonucleotide-based antiviral strategies. Handb. Exp. Pharmacol. 173, 261–287.

Sidwell, R.W., Smee, D.F., 2003. Viruses of the *Bunya*- and *Togaviridae* families: potential as bioterrorism agents and means of control. Antiviral. Res. 57 (1–2), 101–111.

Stein, D., Foster, E., Huang, S.B., Weller, D., Summerton, J., 1997. A specificity comparison of four antisense types: morpholino, 2′-*O*-methyl RNA, DNA, and phosphorothioate DNA. Antisense Nucleic Acid Drug Dev. 7 (3), 151–157.

Strauss, J.H., Strauss, E.G., 1994. The alphaviruses: gene expression, replication, and evolution. Microbiol. Rev. 58 (3), 491–562.

Fig. 5. Antiviral efficacy of PPMO treatment against VEEV in mice. A) Survival of PPMO-treated mice. Nine-week-old NIH Swiss mice were treated with VEEV-specific P7-PPMO (combined VEEV AUG and VEEV 5′+) or the control Scr P7-PPMO at a dose of 40 μg via intranasal (i.n.) route and 160 μg via subcutaneous (s.c.) route at time points pre- (2 doses: −24 h and −4 h, indicated as "+pre") and/or post-infection (5 doses: daily on day +1 through +5, indicated as "+post"). Treatment groups are indicated in the figure legend, as follows: 1) AUG and 5′+ (+pre, +post)/no VEEV: VEEV-specific PPMO at time points prior to (+pre) and following (+post) infection; graph symbol ○, 2) No PPMO/+VEEV: no treatment of VEEV-infected mice; graph symbol +, 3) Scr (+pre, +post)/+VEEV: Scr treatment at pre- and post-infection time points; graph symbol ◆, 4) AUG and 5′+ (+pre, +post)/+VEEV: VEEV-specific PPMO at pre- and post-infection time points; graph symbol ▲, 5) AUG and 5′+ (−pre, +post)/+VEEV: VEEV-specific PPMO at post-infection time points only; graph symbol Δ. On day 0, mice were infected via i.n. route with virulent VEEV (ZPC738) at a dose of 10^3 PFU per animal (groups 2–6). As a control for P7-PPMO toxicity, group 1 was treated with VEEV-specific P7-PPMO in an identical manner as group 4, but was not infected with VEEV. Mice were observed daily and deaths recorded over a 28-day period following infection. B) Infectious virus levels in the tissues of no PPMO or VEEV-specific PPMO-treated mice. Randomly pre-selected mice (N=4 per group) from groups receiving no PPMO treatment (group 2) or VEEV-specific PPMO treatment (groups 4 and 5), described for panel A, were euthanized at 2, 3 and 4 days post-infection (dpi) for harvest of blood, brain and peripheral organs (liver, spleen and lung). Infectious virus levels were determined via plaque assay. The horizontal line depicts the limit of detection. Asterisk (*) indicates that no virus was detected for any organ sample tested in the respective group.

Summerton, J., Weller, D., 1997. Morpholino antisense oligomers: design, preparation, and properties. Antisense Nucleic Acid Drug Dev. 7 (3), 187–195.
Tsiang, M., Weiss, B.G., Schlesinger, S., 1988. Effects of 5′-terminal modifications on the biological activity of defective interfering RNAs of Sindbis virus. J. Virol. 62 (1), 47–53.
Vagnozzi, A., Stein, D.A., Iversen, P.L., Rieder, E., 2007. Inhibition of foot-and-mouth disease virus infections in cell cultures with antisense morpholino oligomers. J. Virol. 81 (21), 11669–11680.
van den Born, E., Stein, D.A., Iversen, P.L., Snijder, E.J., 2005. Antiviral activity of morpholino oligomers designed to block various aspects of Equine Arteritis virus amplification in cell culture. J. Gen. Virol. 86 (Pt 11), 3081–3090.
Vasiljeva, L., Merits, A., Auvinen, P., Kaariainen, L., 2000. Identification of a novel function of the alphavirus capping apparatus. RNA 5′-triphosphatase activity of Nsp2. J. Biol. Chem. 275 (23), 17281–17287.
Wang, E., Barrera, R., Boshell, J., Ferro, C., Freier, J.E., Navarro, J.C., Salas, R., Vasquez, C., Weaver, S.C., 1999. Genetic and phenotypic changes accompanying the emergence of epizootic subtype IC Venezuelan equine encephalitis viruses from an enzootic subtype ID progenitor. J. Virol. 73 (5), 4266–4271.
Weaver, S.C., Ferro, C., Barrera, R., Boshell, J., Navarro, J.C., 2004. Venezuelan equine encephalitis*. Annu. Rev. Entomol. 49, 141–174.
Youngblood, D.S., Hatlevig, S.A., Hassinger, J.N., Iversen, P.L., Moulton, H.M., 2007. Stability of cell-penetrating peptide-morpholino oligomer conjugates in human serum and in cells. Bioconjug. Chem. 18 (1), 50–60.
Yuan, J., Stein, D.A., Lim, T., Qiu, D., Coughlin, S., Liu, Z., Wang, Y., Blouch, R., Moulton, H.M., Iversen, P.L., Yang, D., 2006. Inhibition of coxsackievirus B3 in cell cultures and in mice by peptide-conjugated morpholino oligomers targeting the internal ribosome entry site. J. Virol. 80 (23), 11510–11519.
Zhang, Y.J., Stein, D.A., Fan, S.M., Wang, K.Y., Kroeker, A.D., Meng, X.J., Iversen, P.L., Matson, D.O., 2006. Suppression of porcine reproductive and respiratory syndrome virus replication by morpholino antisense oligomers. Vet. Microbiol. 117 (2–4), 117–129.